

Mapping Dynamic Water Diffusion Process inside Human Brain based on Numerical Solution of the Diffusion Equation

W. Zhan¹, L. Jiang², Y. Yang¹

¹Neuroimaging Research Branch, National Institute on Drug Abuse, NIH, Baltimore, MD, United States, ²Department of Electrical and Computer Engineering, George Washington University, Washington, DC, United States

Introduction

Diffusion tensor imaging (DTI) and beyond-tensor techniques have been developed to quantify the diffusion patterns associated with tissue structures and connectivities [1-3]. However, these diffusion-based MRI techniques provide only static structural information rather than dynamic processes of water diffusion in the tissues. No technique is currently available to estimate the realistic time course of a diffusion process passing through a given region of biological tissue, even though the structural connectivity in the region can be determined. A strategy to address this question is based on the numerical solution of the diffusion equation that governs the dynamic process of the water diffusion. Previous attempts e.g. [4] to employ this strategy had limitations for practical implementation, because only 2-D or partial brain was included into the calculations. In present study, a method is developed to map the 3-D diffusion dynamic process for the whole brain based on a numerical solution of the diffusion equation. The diffusion tensor data are calculated using a regular DTI technique; and the 3-D diffusion equation is discretized and solved by a finite difference method (FDM) with improved numerical stability.

Methods

Diffusion Tensor Imaging. The diffusion-weighted images were acquired using an echo planar imaging (EPI) pulse sequence with the diffusion-sensitizing gradients, and the b value was 1000 s/mm^2 . A total of 30 axial imaging slices of 4 mm thickness with 1 mm gap spacing were prescribed to cover the whole brain (see Fig.1). The in-plane matrix size was 128×128 with an FOV of $24 \times 24 \text{ cm}^2$. TR and TE were 3.0 s and 98 ms, respectively. Diffusion-weighting gradients were applied in 12 independent directions. An EPI image without diffusion-weighting (i.e. $b = 0$) was also acquired as the reference. To suppress noise, each imaging was repeated 4 times to enhance signal-to-noise ratio. The diffusion tensor \mathbf{D} and the fractional anisotropy (FA) index were estimated according to [2].

Diffusion Equation. The dynamic process of an ideal diffusion is governed by the diffusion equation [1], i.e. $\frac{\partial C}{\partial t} = \nabla \cdot \mathbf{D} \nabla C$, where C is concentration of the diffusive medium, and \mathbf{D} is the local diffusion tensor. The operator ∇C represents the concentration gradient, whereas $\nabla \cdot$ denotes the divergent of the diffusion flux density $\mathbf{D} \nabla C$. Using the finite difference method (FDM) approximations to replace the derivatives, the diffusion equation can be equivalently written as a discrete form $C^{n+1} - C^n = \mathbf{A} \cdot C^n$, where C^n is a vector comprised of all the concentration values in the calculation domain, while \mathbf{A} is a sparse matrix incorporating all the calculation parameters and diffusion tensors in the domain. Boundary conditions were specified as equivalent to assume that (a) the brain is immersed in a solution of zero concentration, and (b) water diffusion at the boundaries of the calculation domain is balanced.

Crank-Nicholson Scheme. Given an initial condition C^0 , a time series of the numerical solution can be obtained from the iteration i.e. $C^{n+1} = (\mathbf{I} + \mathbf{A}) \cdot C^n$. A Crank-Nicholson scheme [5] was implemented to significantly enhance the numerical stability based on a temporal averaging approximation. The final iteration scheme was $C^{n+1} = (\mathbf{I} - \mathbf{A})^{-1} \cdot (\mathbf{I} + \mathbf{A}) \cdot C^n$. The initial condition was specified by a seed region in corticospinal tract (CST) (Fig.1) identified by the FA map. The initial concentration was 1 for the seed voxels in the region while 0 for all others.

Results and Discussions

The dynamic diffusion process is illustrated in Fig. 2. The calculated concentration distributions are plotted for successive 6 diffusion time points at 0, 3, 6, 9, 12 and 15 minutes. The concentration distribution is represented by yellow contour curves overlaid on the corresponding T2-weighted brain images aligned to the seed region. The 5 enclosed contour curves (outwards) denote the relative concentrations of 0.833, 0.667, 0.500, 0.333 and 0.167 with respect to the current peak concentration at the center of the contours. It is shown that the concentration distribution quickly spreads to the whole brain as a function of the diffusion time, while the peak concentration spot stays at approximately the same location as the initial seed. The contour curves spread at a higher rate during the initial period of the diffusion process, while the rate gradually slows down with diffusion time. The concentration contours move slightly faster in the superior direction. This phenomenon is due to the fact that the CST seed region is located in an inferior part of the brain with a shorter distance to the boundary of the brain (dashed curve in Fig. 1), thus the boundary condition may have stronger effects on the concentration distribution. In Fig.3, the absolute peak concentration measured at the seed region is illustrated in the semi-logarithm plot (black solid curve) with respect to the diffusion time. The peak concentration dramatically decreases from 1 during the first 2 minutes of the diffusion process until it reaches 10^{-2} , after which the decay rate becomes moderately stable. The dashed curves of color blue, magenta, red and green represent the dynamic concentration changes measured at nearby voxels at distances of 5, 10, 15 and 20 (mm), respectively, from the seed region. As illustrated, the concentration at an "off-seed point" (away from the seed) starts from 0 and quickly increases and approaches its maximum around 1~2 minutes of diffusion. After reaching the maximum, the concentration begins to decrease at a rate slightly lower than that of the seed region. Given sufficiently long diffusion time, the concentrations at both the seed and off-seed regions become convergent. It is also demonstrated that the concentration maximum has a relative higher value and is reached earlier for the off-seed point that is closer to the seed region.

References

[1] Thomas et al, Phys. Med. Biol. 2000; 45: R79-R138. [2] Le Bihan et al, JMRI 2001; 13:534-546. [3] Zhan et al, MRM 2003; 49:1077-1088. [4] Mc Queen et al, ISMRM 1996, 193. [5] Teukolsky, Phys. Rev. D., 2000; Art. #087501.

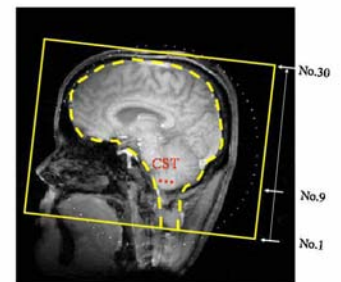


Fig.1 The boundaries and the initial region

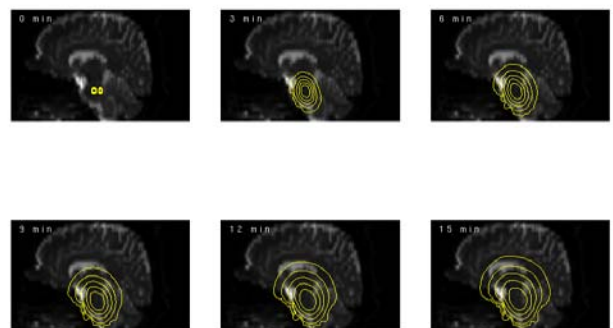


Fig.2 The sagittal view of the diffusion process from the initial region at CST.

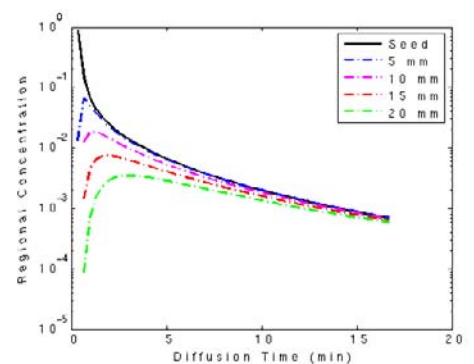


Fig.3 The time course of the absolute concentrations measured at seed and off-seed regions.